First constraints on cosmic 21cm signal with the uGMRT - Lessons learnt from ELAIS-N1 observations

Rashmi Sagar

Department of Astronomy, Astrophysics and Space Engineering (DAASE)
Indian Institute of Technology Indore

In collaboration with Abhirup Datta, Arnab Chakraborty, and members from CD/EoR collaboration of SKAIC

Cosmology in the ALPS, 18 March, Switzerland, 2026

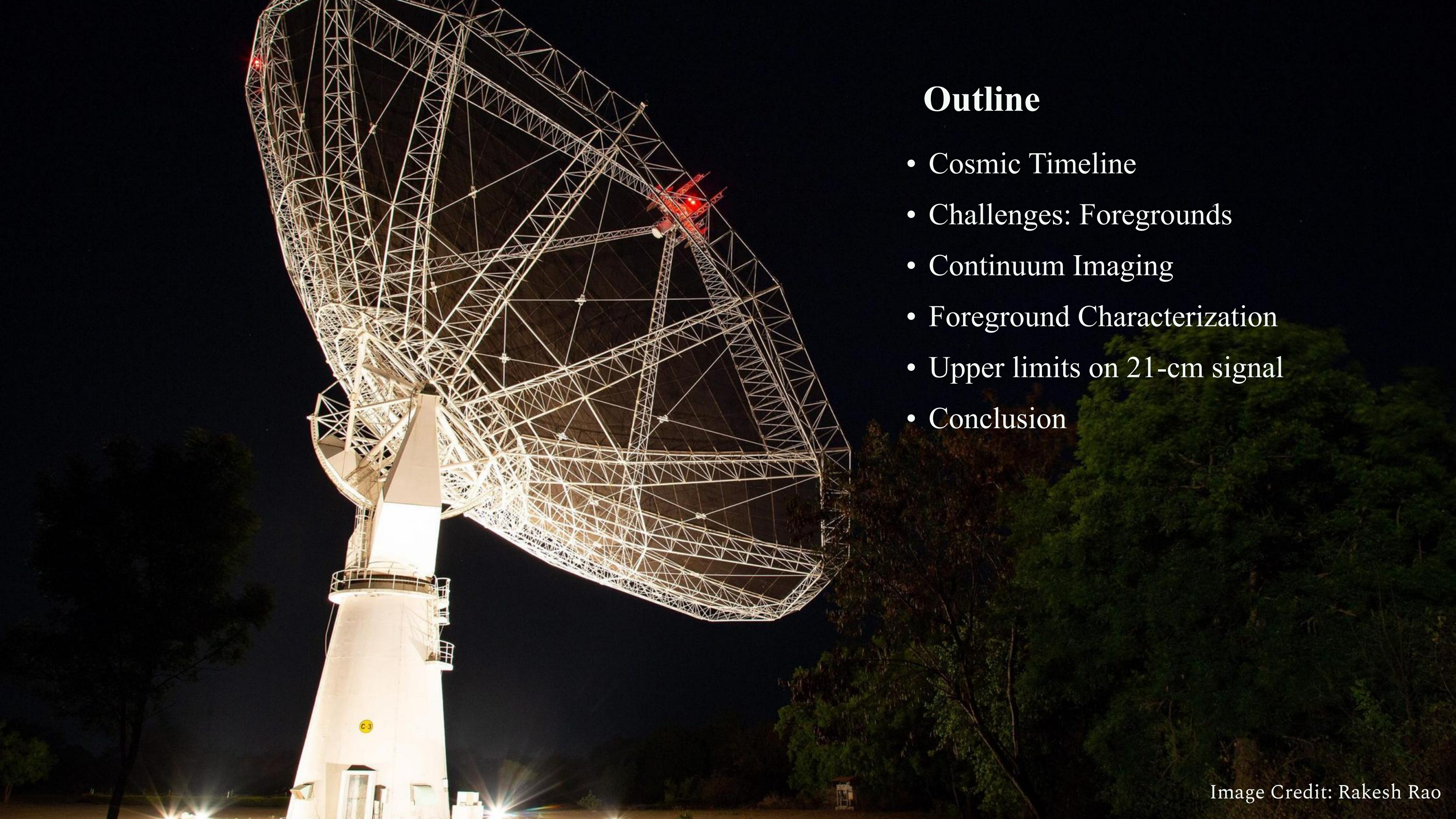

Outline

- Cosmic Timeline
- Challenges: Foregrounds
- Continuum Imaging
- Foreground Characterization
- Upper limits on 21-cm signal
- Conclusion

Image Credit: Rakesh Rao

Image Credit: NAOJ

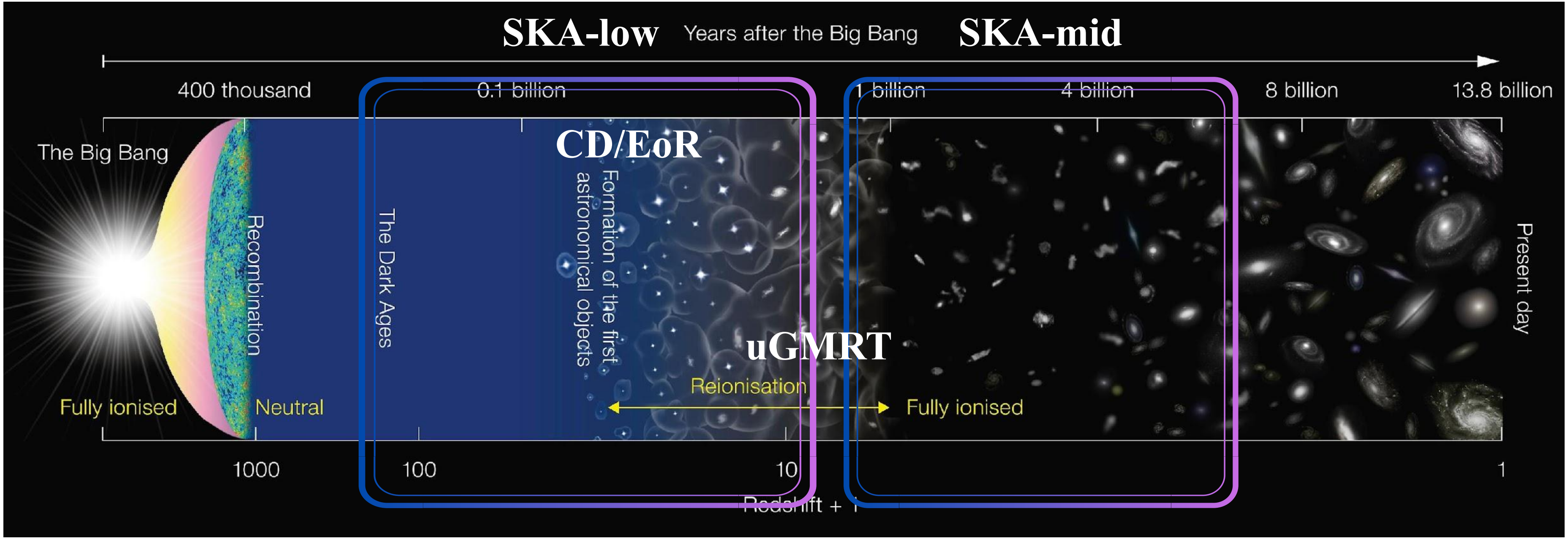

T_γ

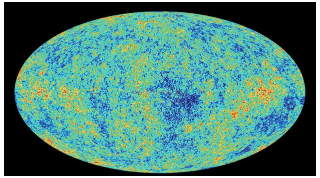

CMB

T_g

T_S

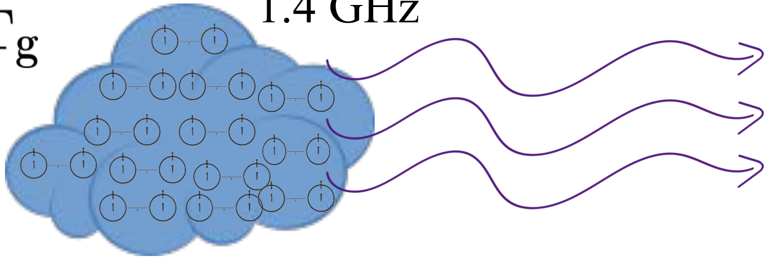

Biggest Challenge: Foregrounds

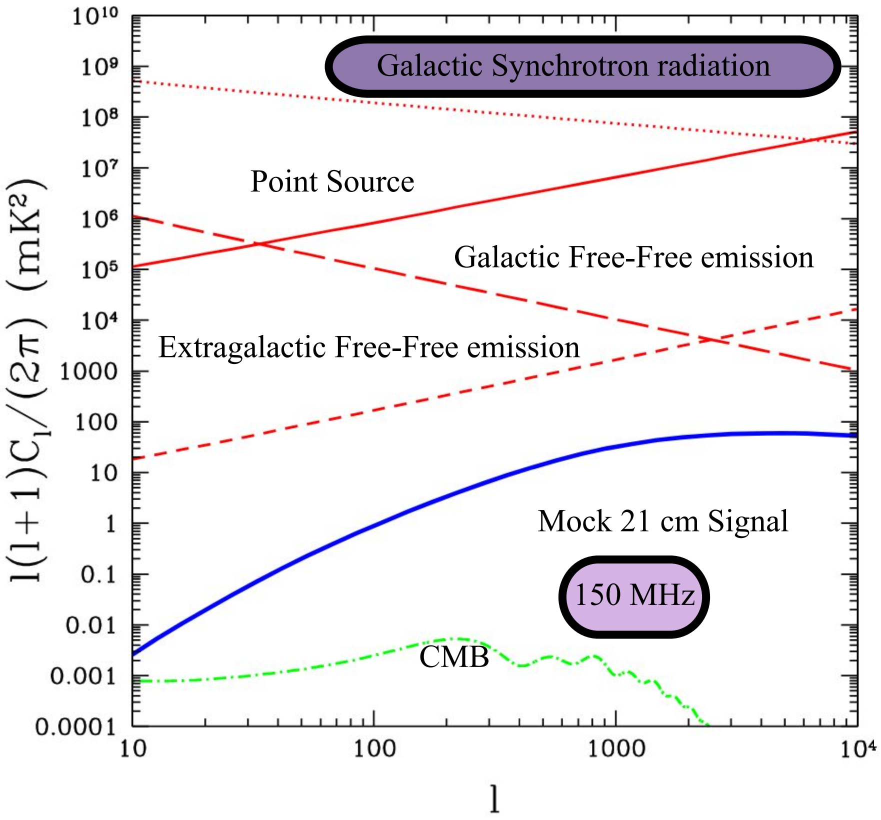

Santos et al., 2005

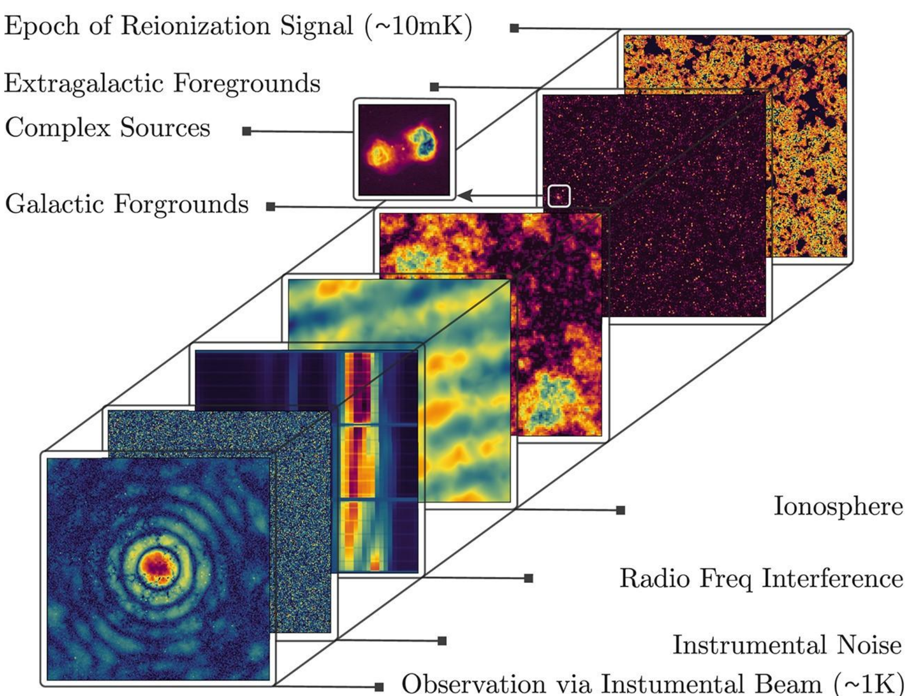

Signal + Foreground at 150 MHz

Chokshi et al. 2024

Current Generation Low-Frequency Radio Interferometers: High-z

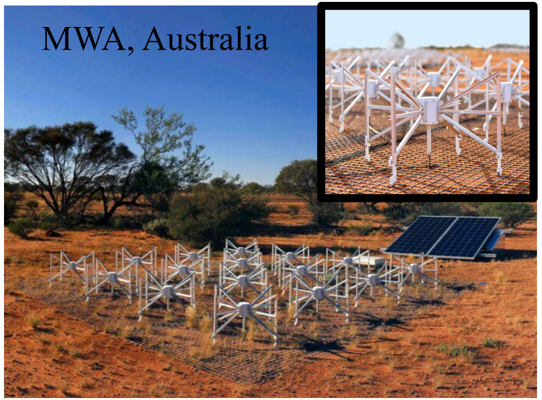

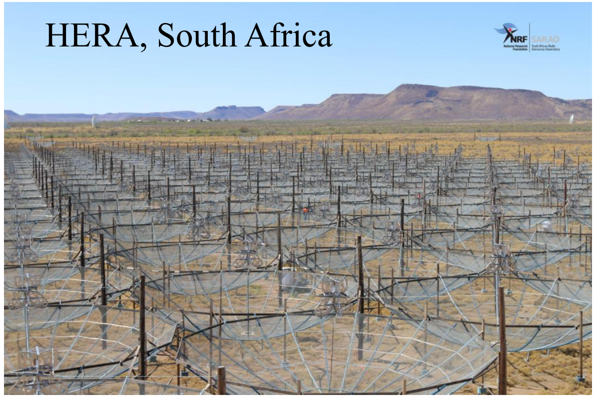

Motivation

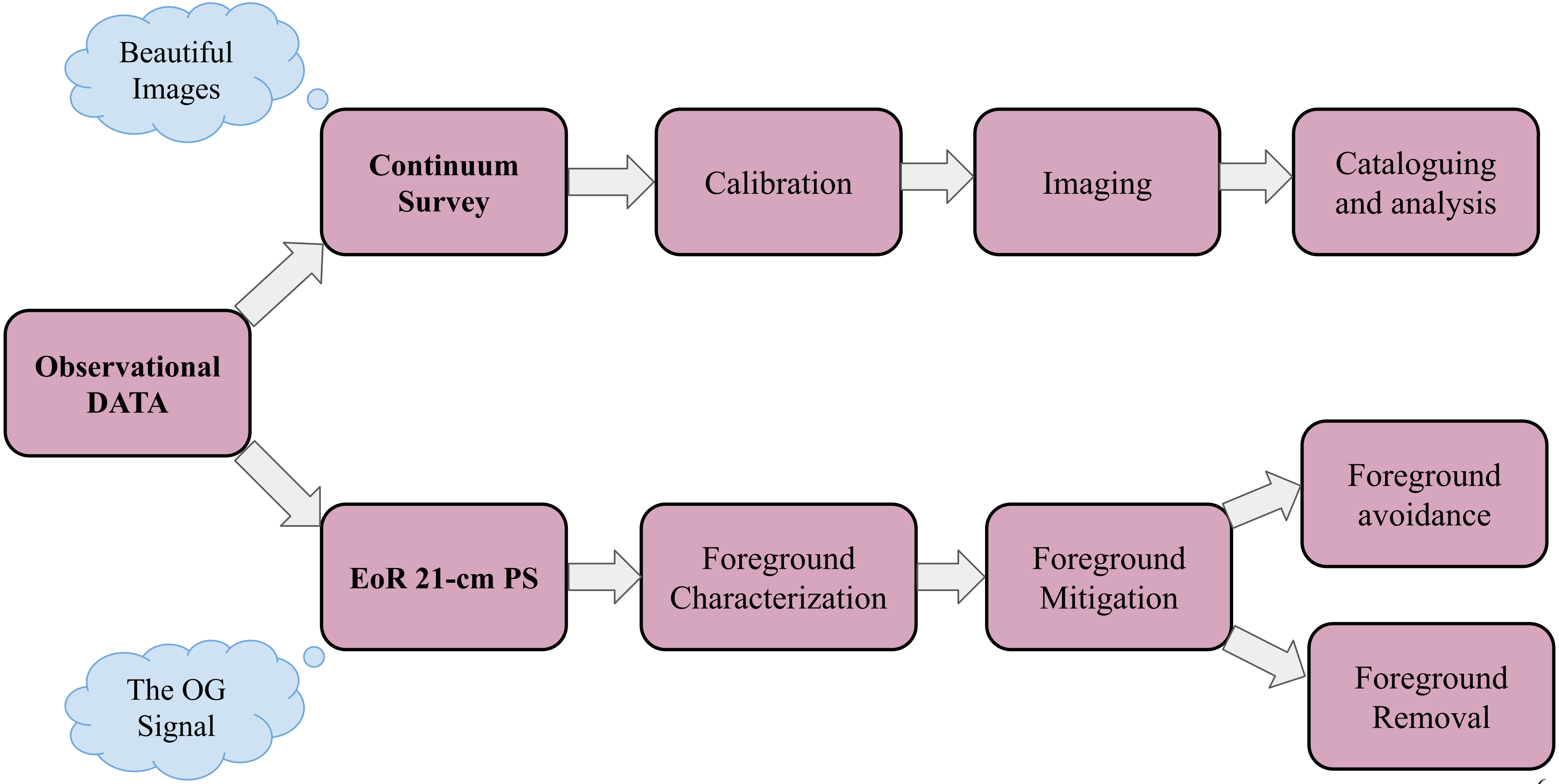
Beautiful Images
Continuum Survey
Calibration
Imaging
Cataloguing and analysis
Observational DATA
EoR 21-cm PS
Foreground Characterization
Foreground Mitigation
Foreground avoidance
Foreground Removal
The OG Signal

Observational INFO

Total Observation Time	32 hours
Frequency	183MHz
Bandwidth	120 - 250 MHz
Integration Time	5.37sec
Number of Channels	8192
Frequency Resolution	24 KHz
Target field $(\alpha, \delta)_{2000}$	$(16^h10^m1^s, +54°30'36")$
Working Antennas	27

Pointing centres	$13^h31^m08^s$ $+30^d30^m32^s$ (3C286)
	$15^h49^m17^s$ $+50^d38^m05^s$ (J1549+506)
	$16^h10^m01^s$ $+54^d30^m36^s$ (ELAIS N1)
	$01^h37^m41^s$ $+33^d09^m35^s$ (3C48)

Sagar et al., 2025 (10.1093/mnras/staf1922)

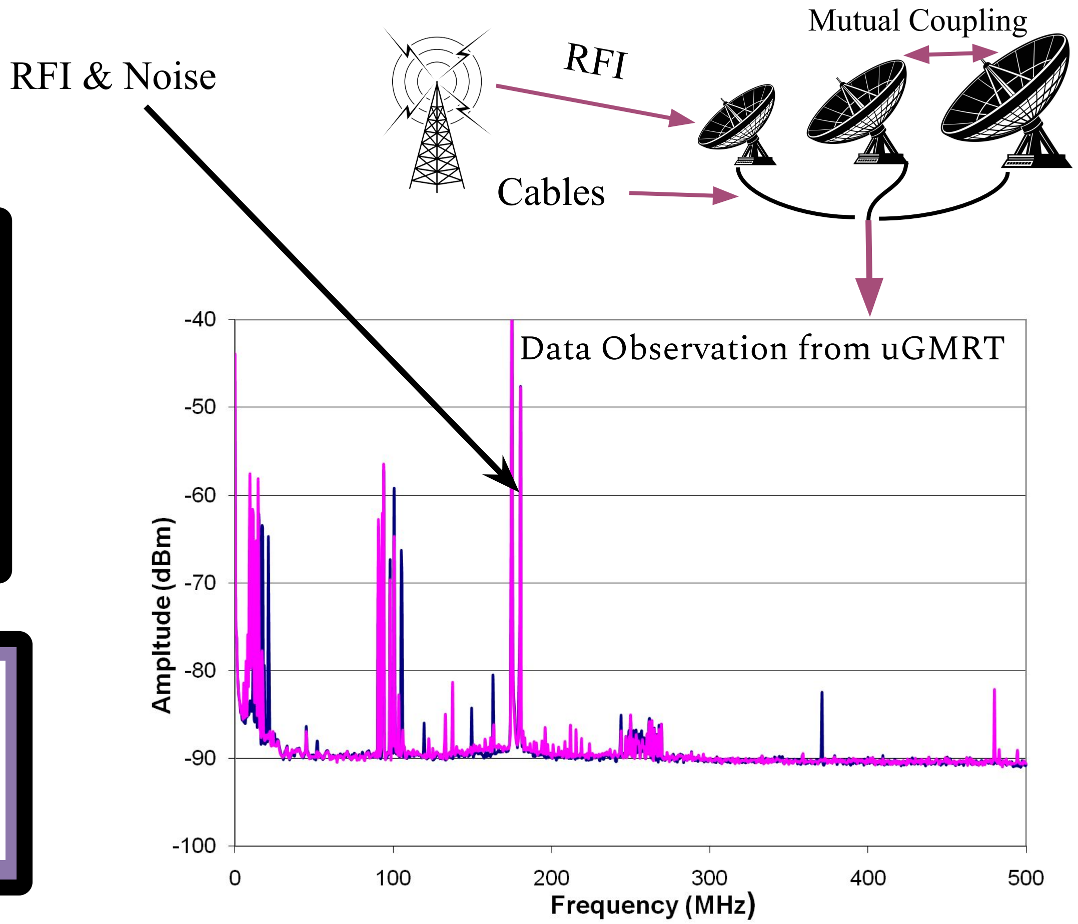

Raybole et al. 2010

Direction-Dependent Calibration : SPAM

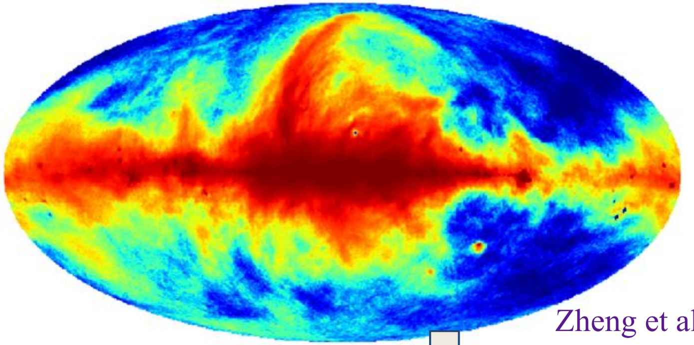

Zheng et al. 2017

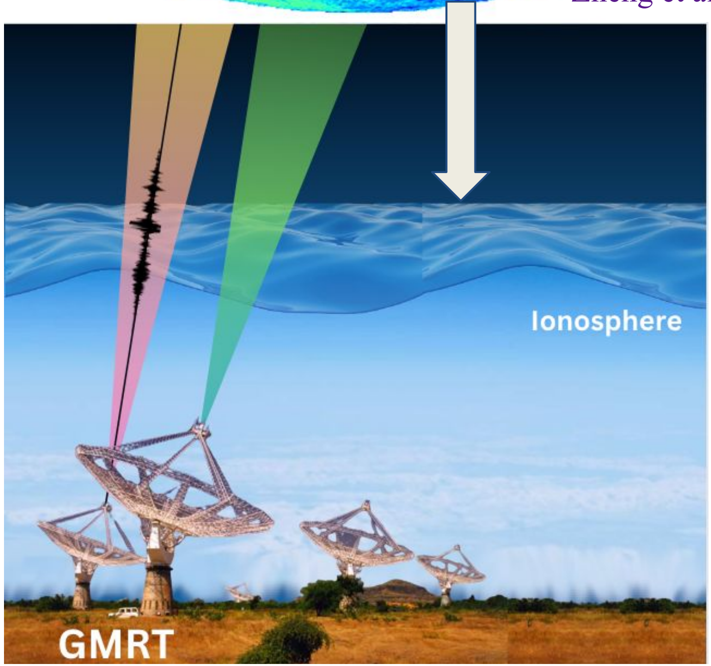

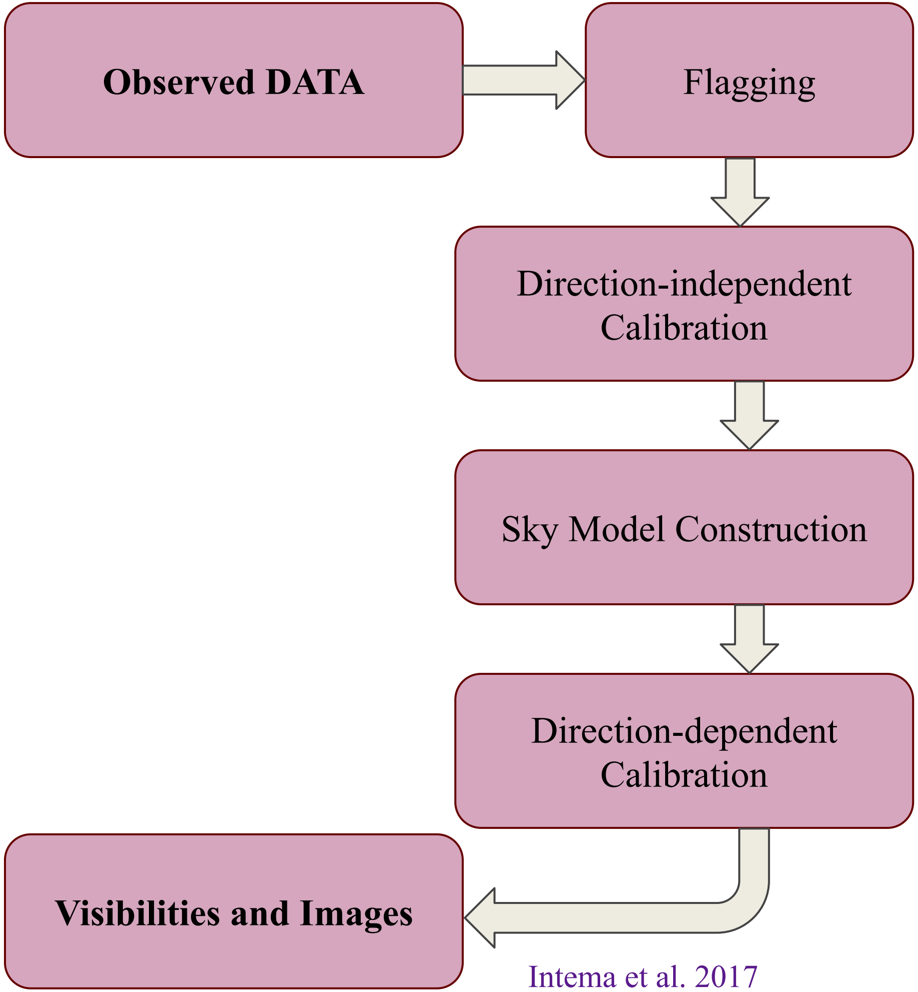

Intema et al. 2017

Results from Individual Nights of Observations

-Role of differential RFI and ionospheric conditions

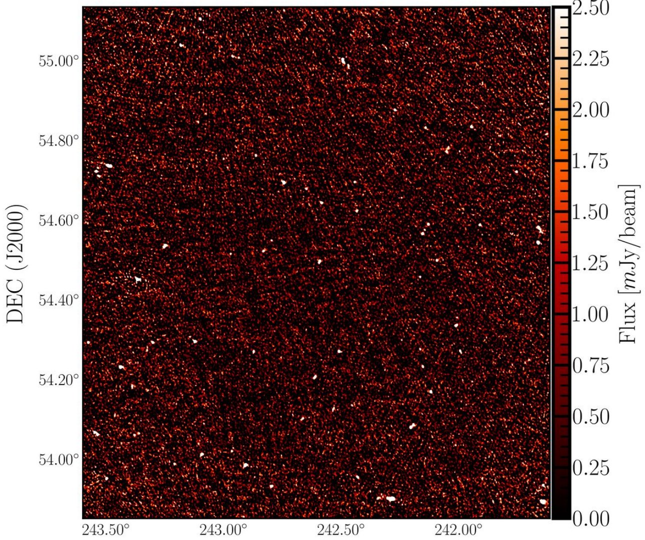

Single DAY

RMS Noise: 721 μJy/beam

DAY - 1

RMS Noise: 290 μJy/beam

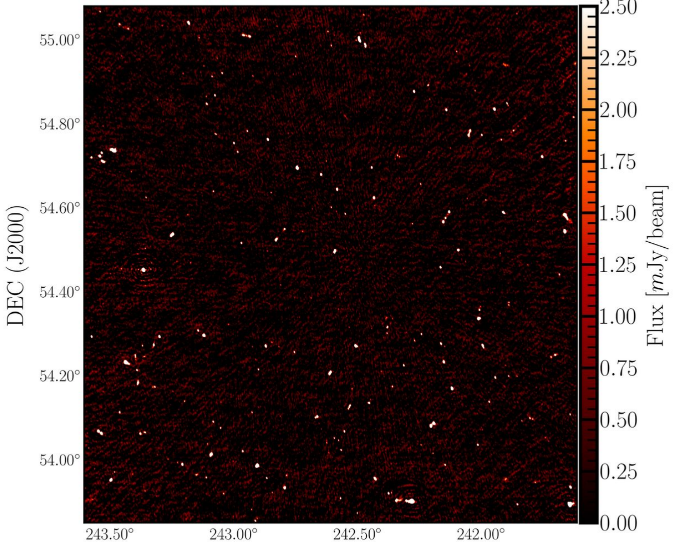

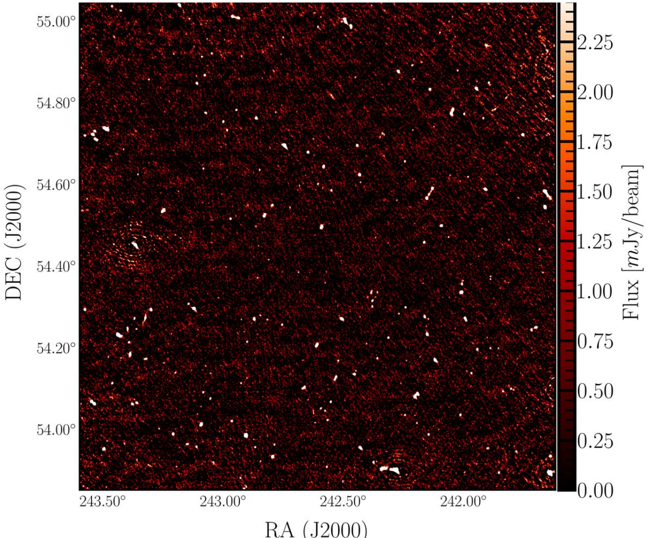

DAY - 2

RMS Noise: 498 μJy/beam

DAY - 3

RMS Noise: 280 μJy/beam

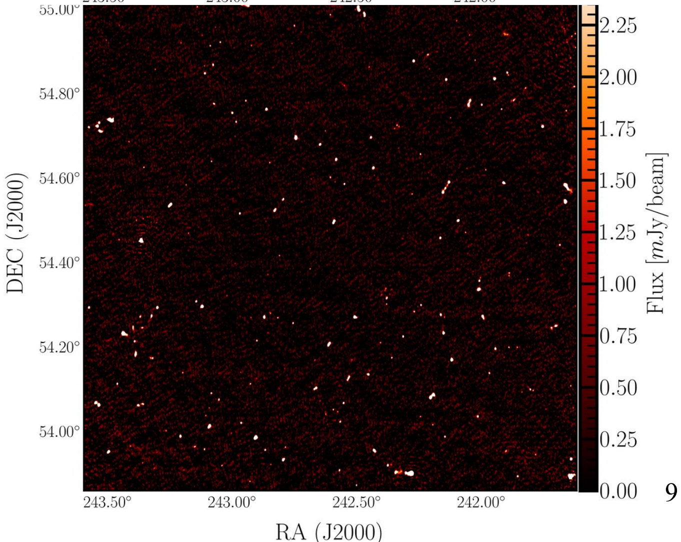

Sagar et al., 2025

(10.1093/mnras/staf1922)

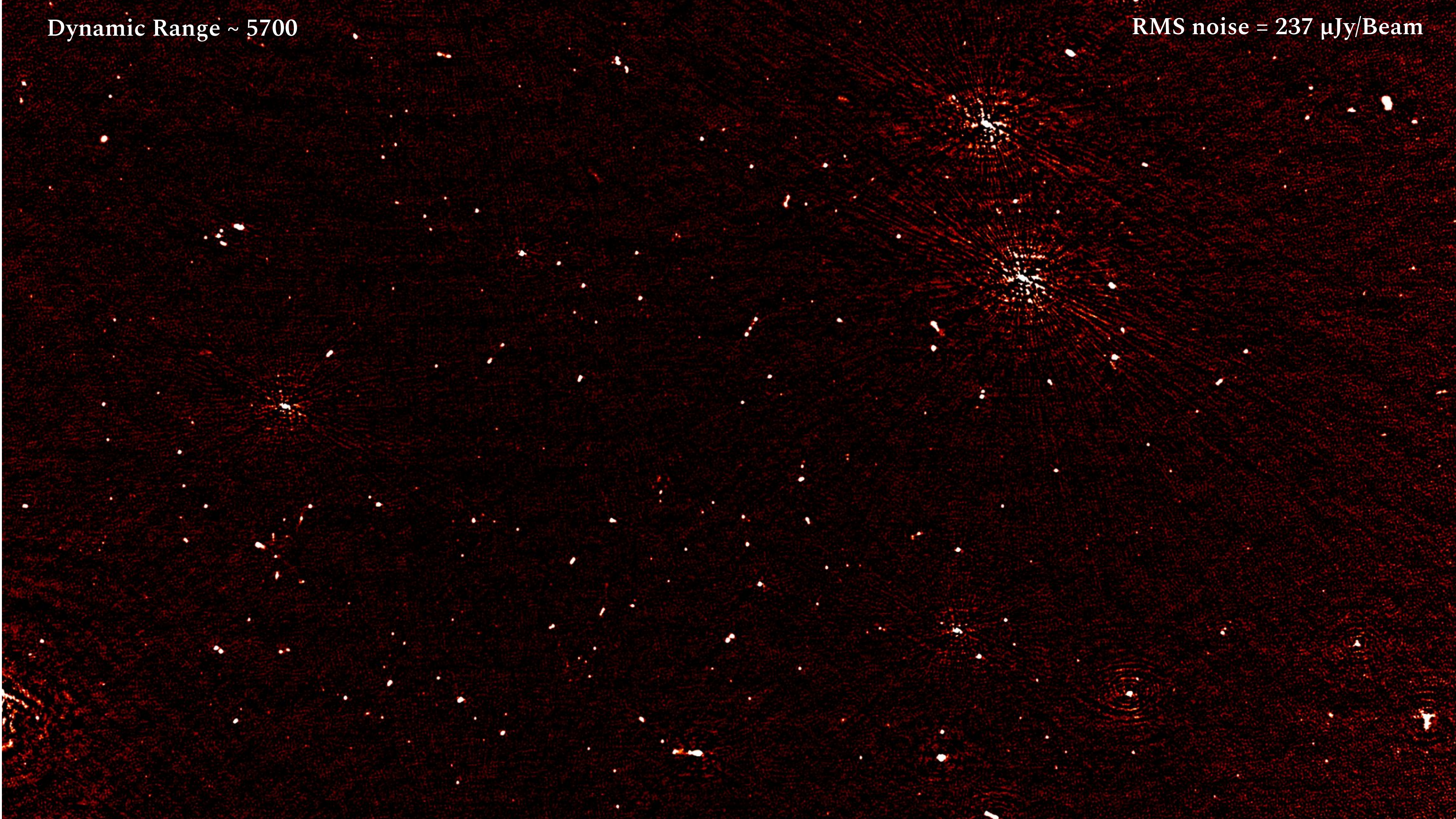
Dynamic Range ~ 5700
RMS noise = 237 μJy/Beam

Source Classification

1027 Sources

$$\ln\left(\frac{S_{int}}{S_{peak}}\right) > 3\sqrt{\left(\frac{\sigma_S}{S_{int}}\right)^2 + \left(\frac{\sigma_{peak}}{S_{peak}}\right)^2}$$

Franzen et al. 2019

Resolved Sources = 301 (Red)

Unresolved sources = 726 (Green)

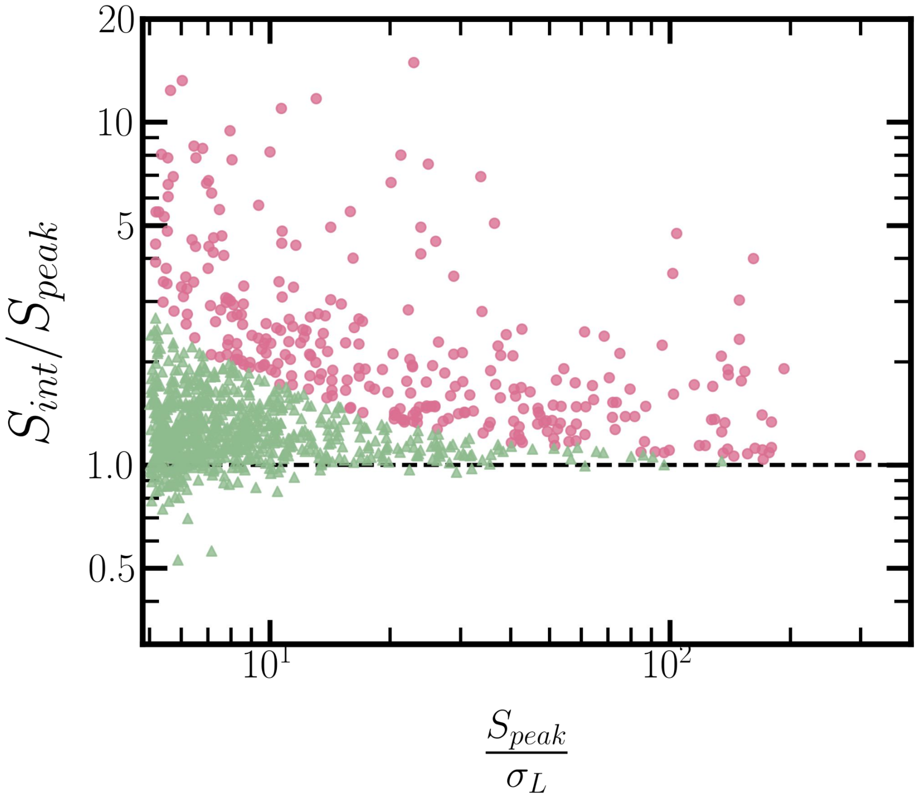

Sagar et al., 2025

(10.1093/mnras/staf1922)

Flux offset

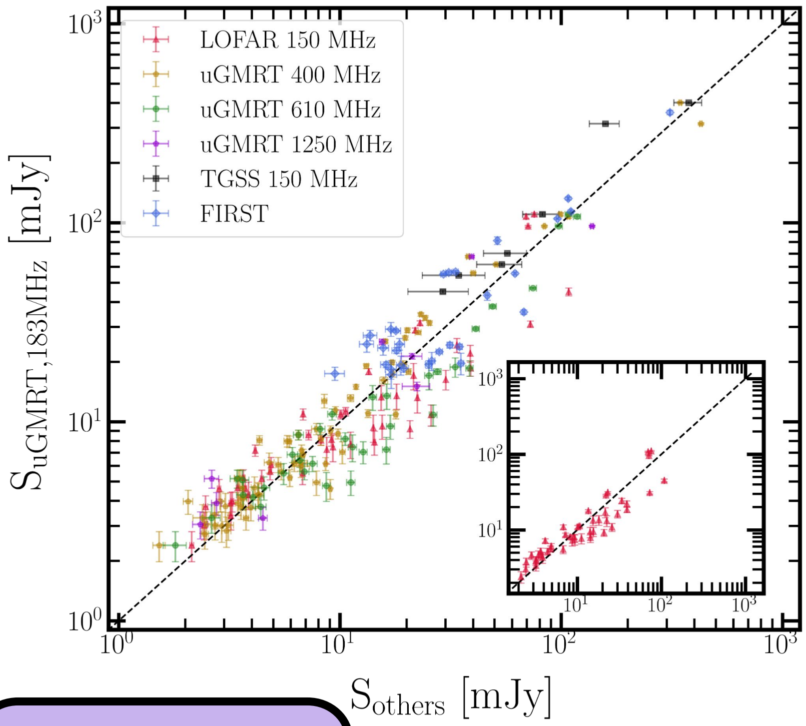

Mean offset :

1.4 GHz FIRST = 0.88

150 MHz LOFAR = 1.07

Source counts

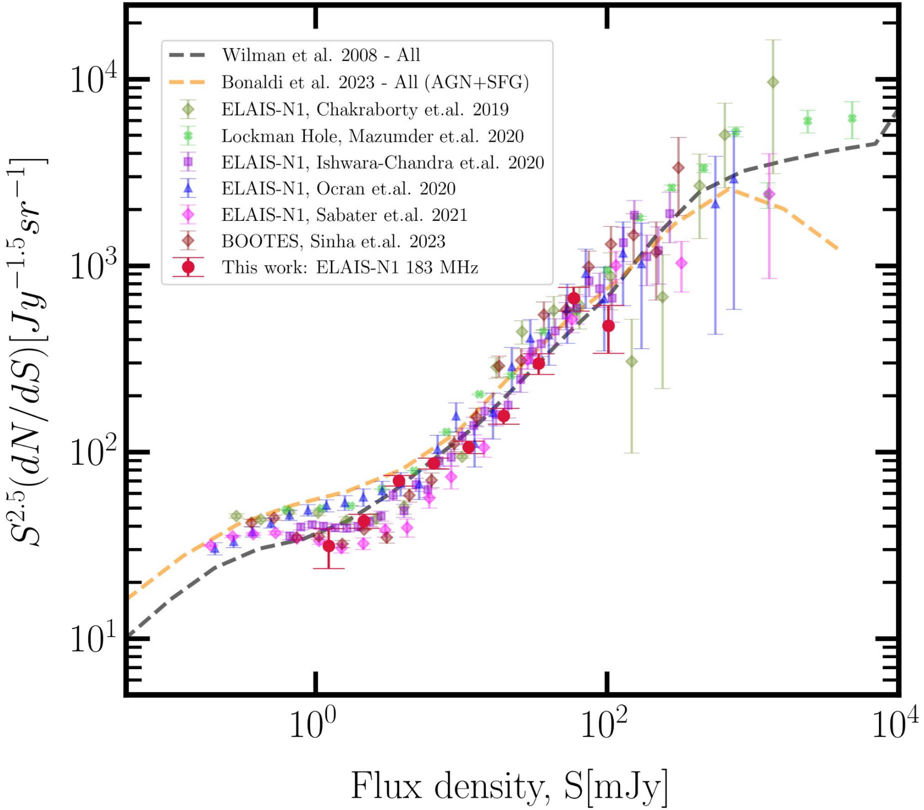

Sagar et al., 2025

(10.1093/mnras/staf1922)

Galactic Diffuse Emission Angular Power Spectra - Visibility & Imaging

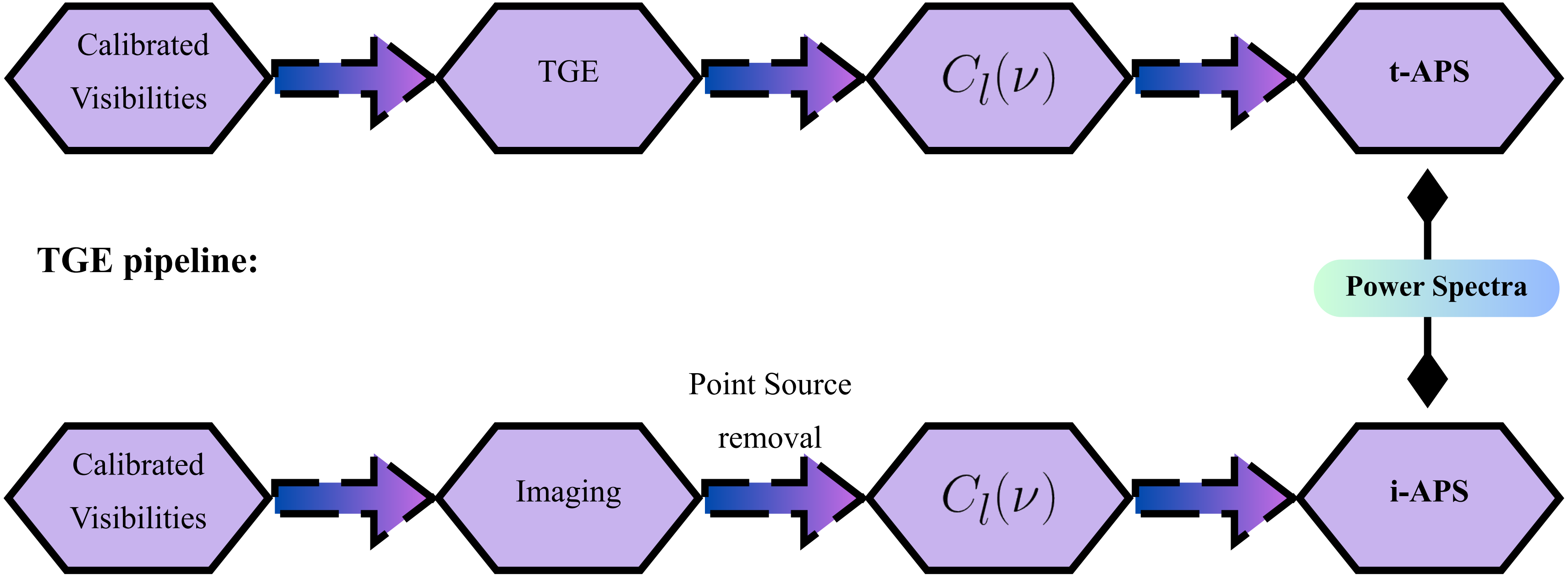

Imaging pipeline:

Band-2 - Power law of DGSE - i-APS vs t-APS

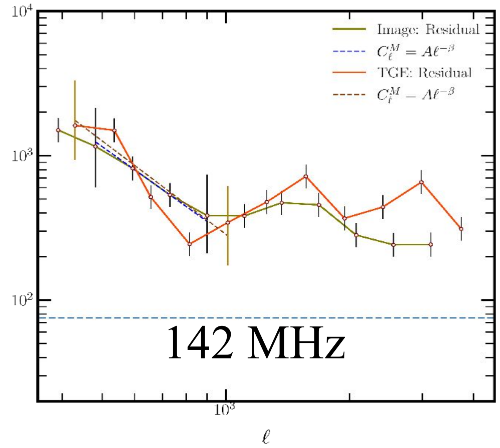

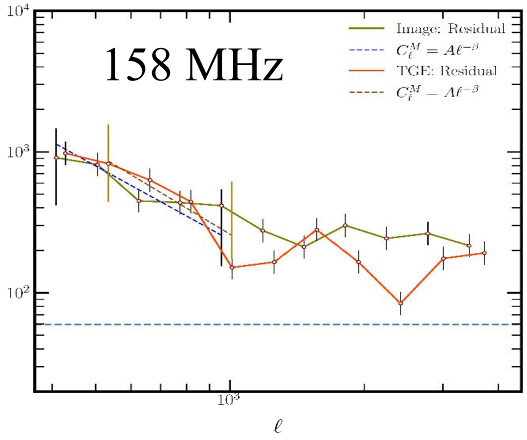

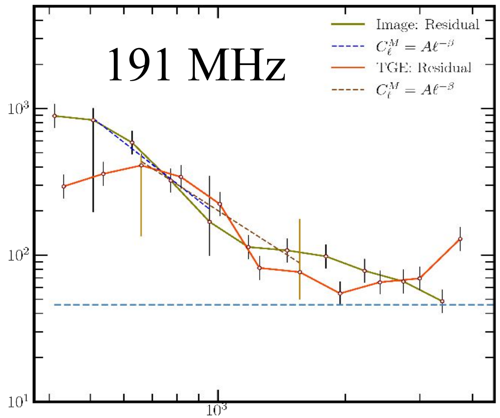

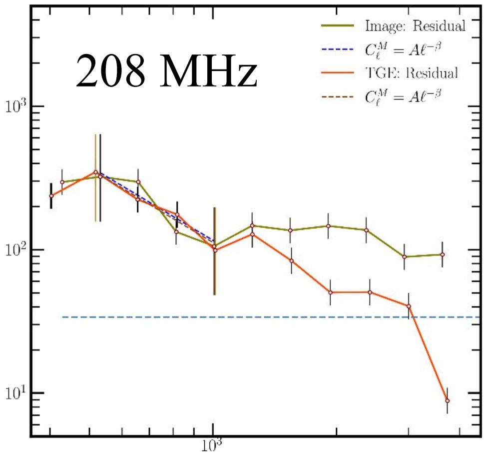

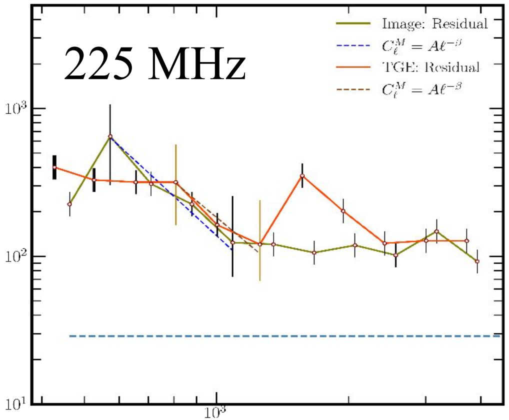

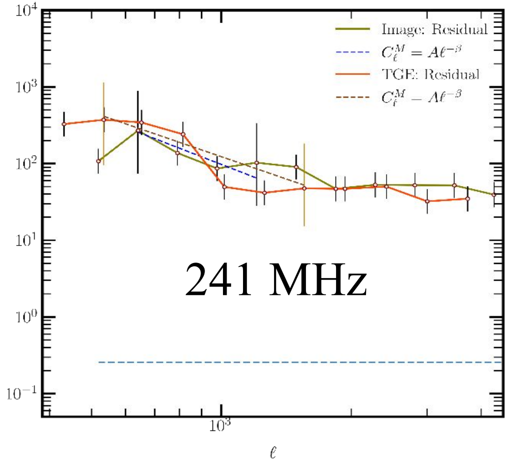

Sagar et al., 2025 (10.1093/mnras/staf1922)

Band-3 - Power law of DGSE - i-APS vs t-APS

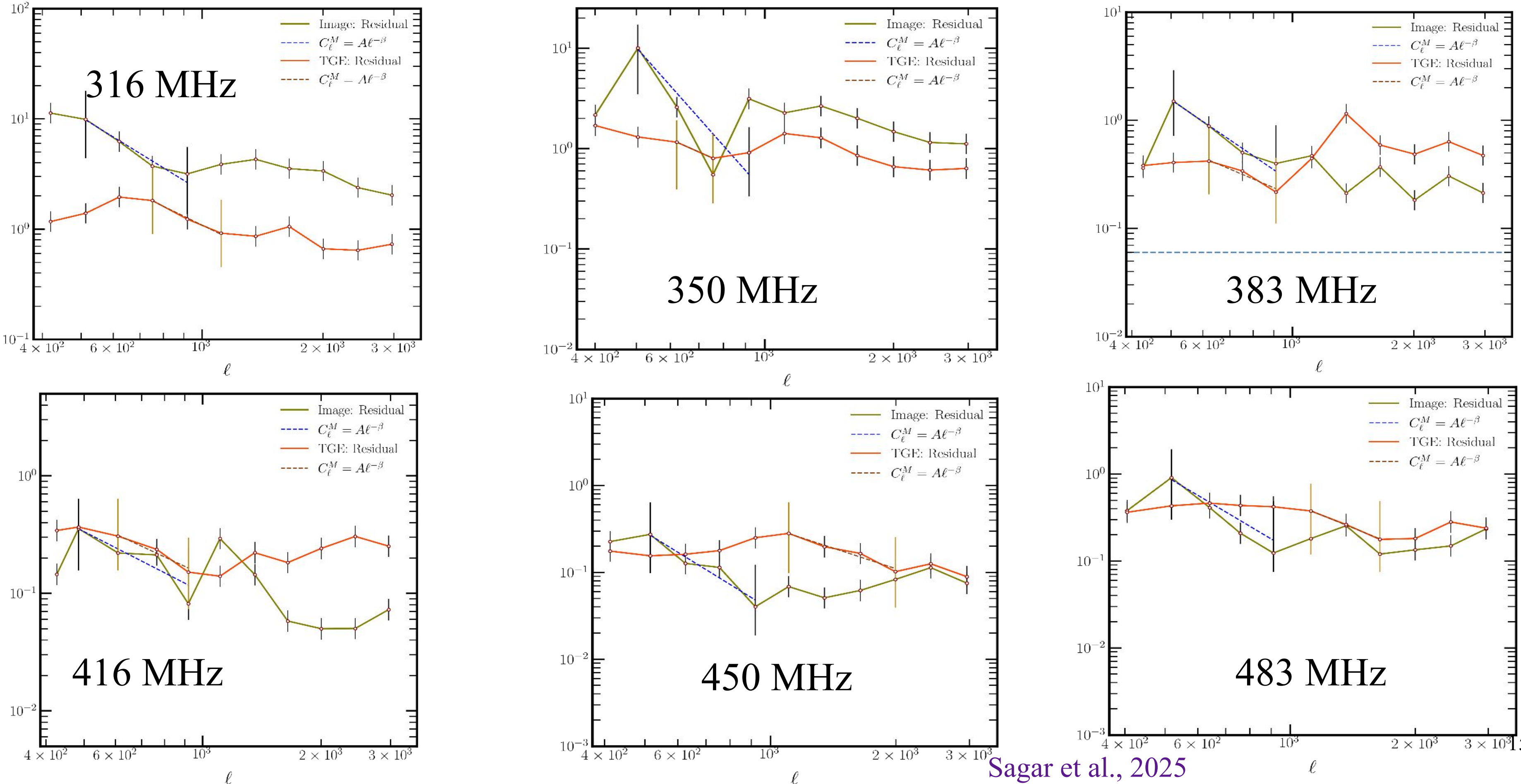

Sagar et al., 2025

Broken Power-law over wideband (120 - 500 MHz)

Best-fit parameters for single power law:

$$\mathbf{C_M^\ell} = \mathbf{A_{150}}\left(\frac{\mathbf{1000}}{\ell}\right)^\beta$$

A = 143.82 ± 14.58 mK^2

alpha = 4.08 ± 0.07

χ^2 : large i.e. > 5

Best-fit parameters for broken power law:

$$C_\ell(\nu) = \begin{cases} A\left(\frac{\nu}{\nu_{\rm break}}\right)^{-2\alpha_1} & \text{if } \nu \leq \nu_{\rm break} \\ A\left(\frac{\nu}{\nu_{\rm break}}\right)^{-2\alpha_2} & \text{if } \nu \geq \nu_{\rm break} \end{cases}$$

A = 112.25 ± 20.88 mK^2

nu_break = 230 ± 5 MHz

alpha_1 = 1.27 ± 0.15

alpha_2 = 5.37 ± 0.27

χ^2 : 1.15

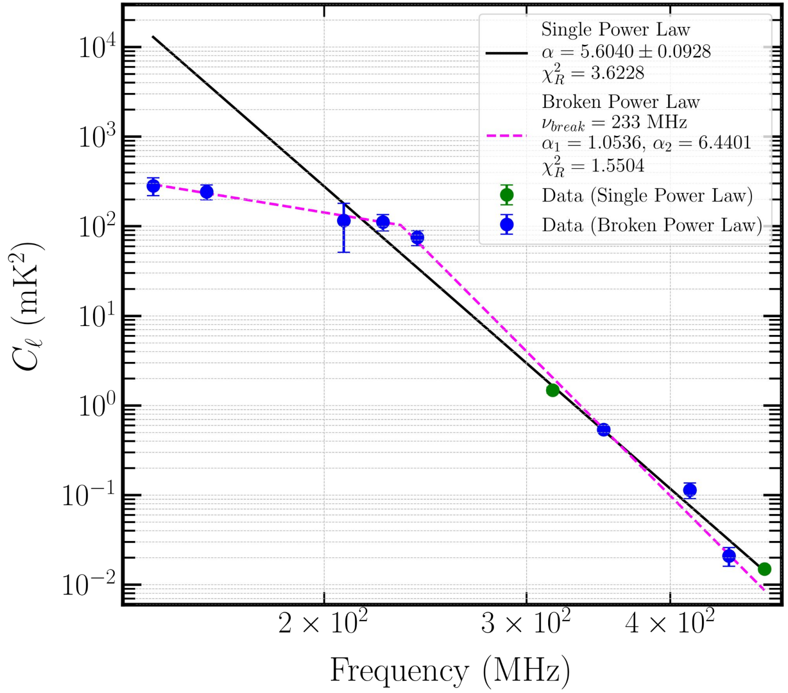

Sagar et al., 2025

(10.1093/mnras/staf1922)

Parameters of Power law of DGSE - i-APS and t-APS

ν (MHz)	i-APS A (mK^2)	i-APS β	i-APS $\ell_{min} - \ell_{max}$	t-APS A (mK^2)	t-APS β	t-APS $\ell_{min} - \ell_{max}$
142	283.002 ± 63.509	2.028 ± 0.265	390 – 900	285.641 ± 140.413	2.147 ± 0.664	429 – 1010
158	243.802 ± 48.148	1.744 ± 0.347	407 – 955	260.794 ± 63.639	1.901 ± 0.464	533 – 1010
191	201.547 ± 3.615	2.253 ± 0.265	507 – 955	201.570 ± 25.139	1.852 ± 0.369	659 – 1561
208	185.439 ± 10.333	1.712 ± 0.984	530 – 1007	112.145 ± 10.333	1.713 ± 0.169	517 – 1012
225	138.221 ± 19.730	2.737 ± 0.744	572 – 1088	183.368 ± 16.955	2.476 ± 0.489	806 – 1255
241	90.197 ± 24.168	2.179 ± 0.499	640 – 1206	123.004 ± 32.174	1.932 ± 0.499	533 – 1556
316	2.186 ± 0.461	2.244 ± 0.275	512 – 918	1.087 ± 0.029	1.779 ± 0.120	751 – 1114
350	0.366 ± 0.026	2.388 ± 0.325	503 – 917	0.472 ± 0.039	1.888 ± 0.464	621 – 755
383	0.266 ± 0.030	2.543 ± 0.189	507 – 909	0.174 ± 0.028	2.353 ± 0.366	620 – 909
416	0.102 ± 0.020	1.716 ± 0.557	483 – 919	0.144 ± 0.020	1.562 ± 0.341	609 – 919
450	0.038 ± 0.005	2.959 ± 0.742	514 – 919	0.328 ± 0.019	1.574 ± 0.179	1105 – 1993
483	0.133 ± 0.021	2.839 ± 0.984	517 – 1121	0.471 ± 0.009	1.935 ± 0.071	1121 – 2001

Notes. The parameters A and β correspond to the amplitude and spectral index in the power law, respectively. The ℓ_{min} and ℓ_{max} represent the multipole range in which GDSE dominates.

Sagar et al., 2025

(10.1093/mnras/staf1922)

Technique for upper limit of 21-cm signal

- **Foreground Avoidance** – Ignores contaminated modes in Fourier space (EoR window approach).

- **Foreground Subtraction** – Models and removes foregrounds before power spectrum estimation. Example - PCA, GPR.

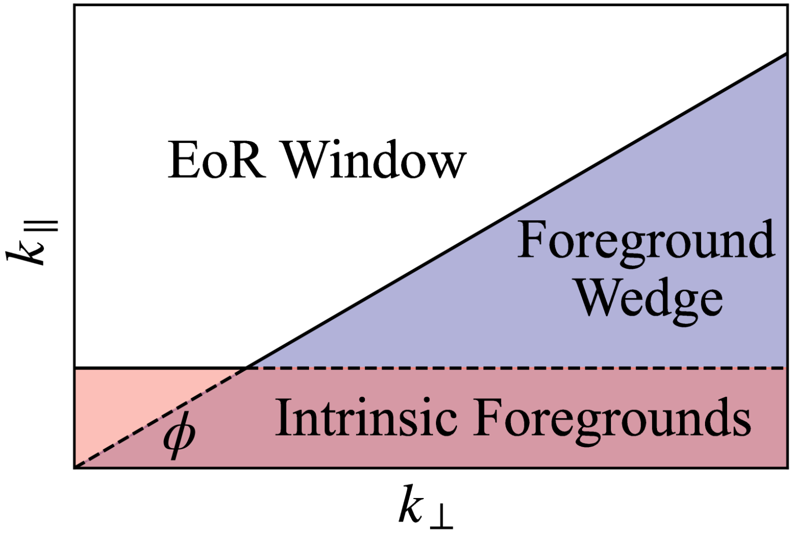

Kennedy et al. 2024

Upper limit on 21-cm signal with other telescopes at High - z

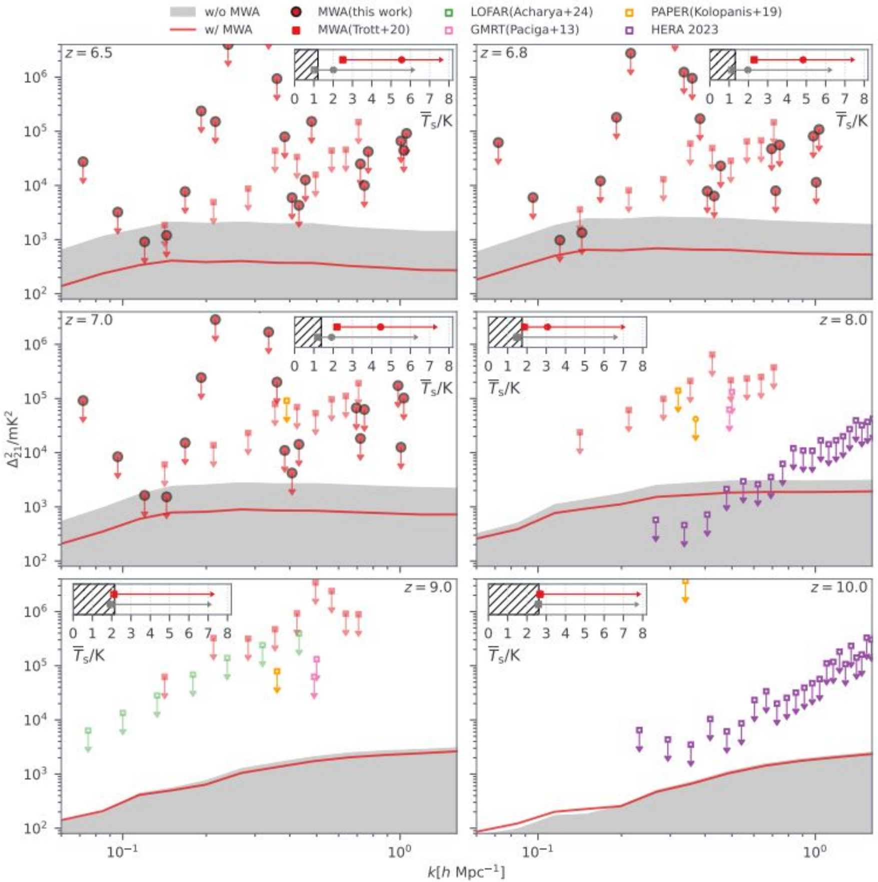

z = 6.5-7.0
Total time = 268 hr

MWA

Nunhokee et al., 2025

Upper limit on 21-cm signal with other telescopes at High - z

LOFAR Multi-redshift upper - limit

Mertens et al., 2025

z = 8-10
Total time = 141 hr

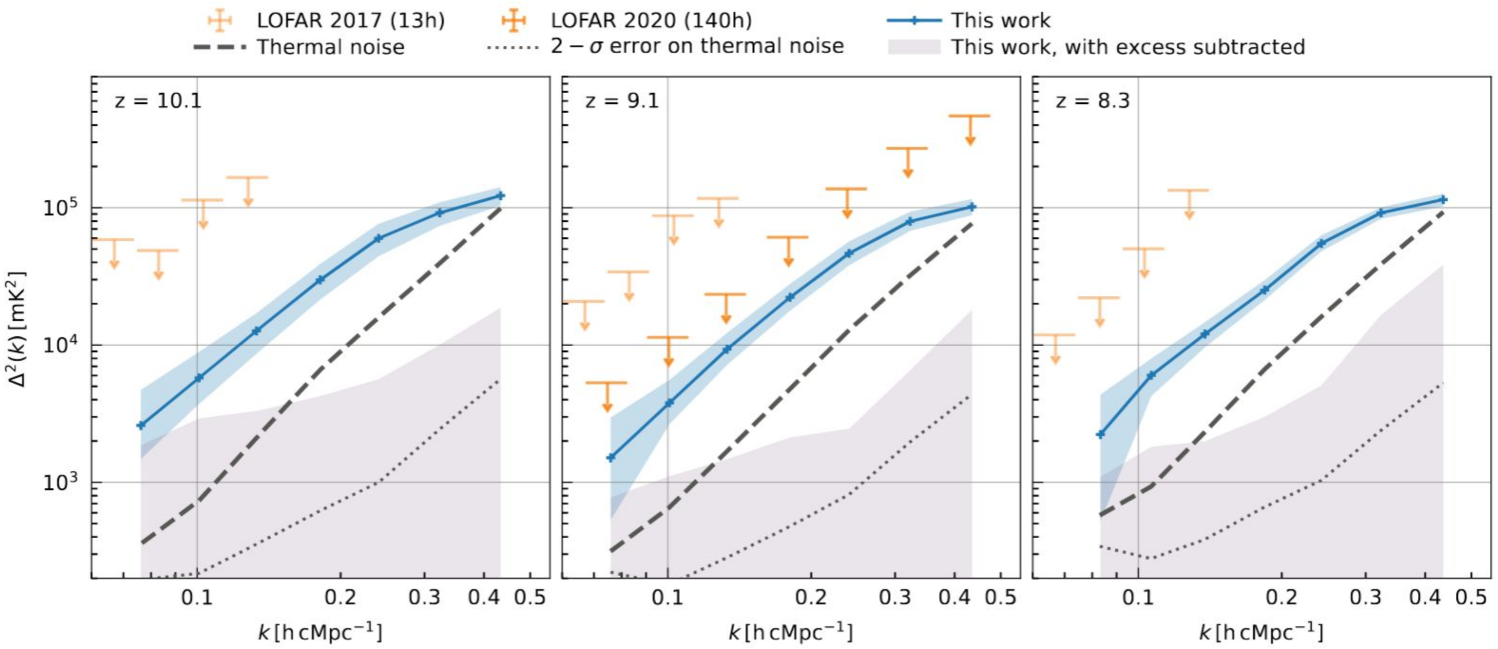

Upper limit on 21-cm signal with other telescopes at High - z

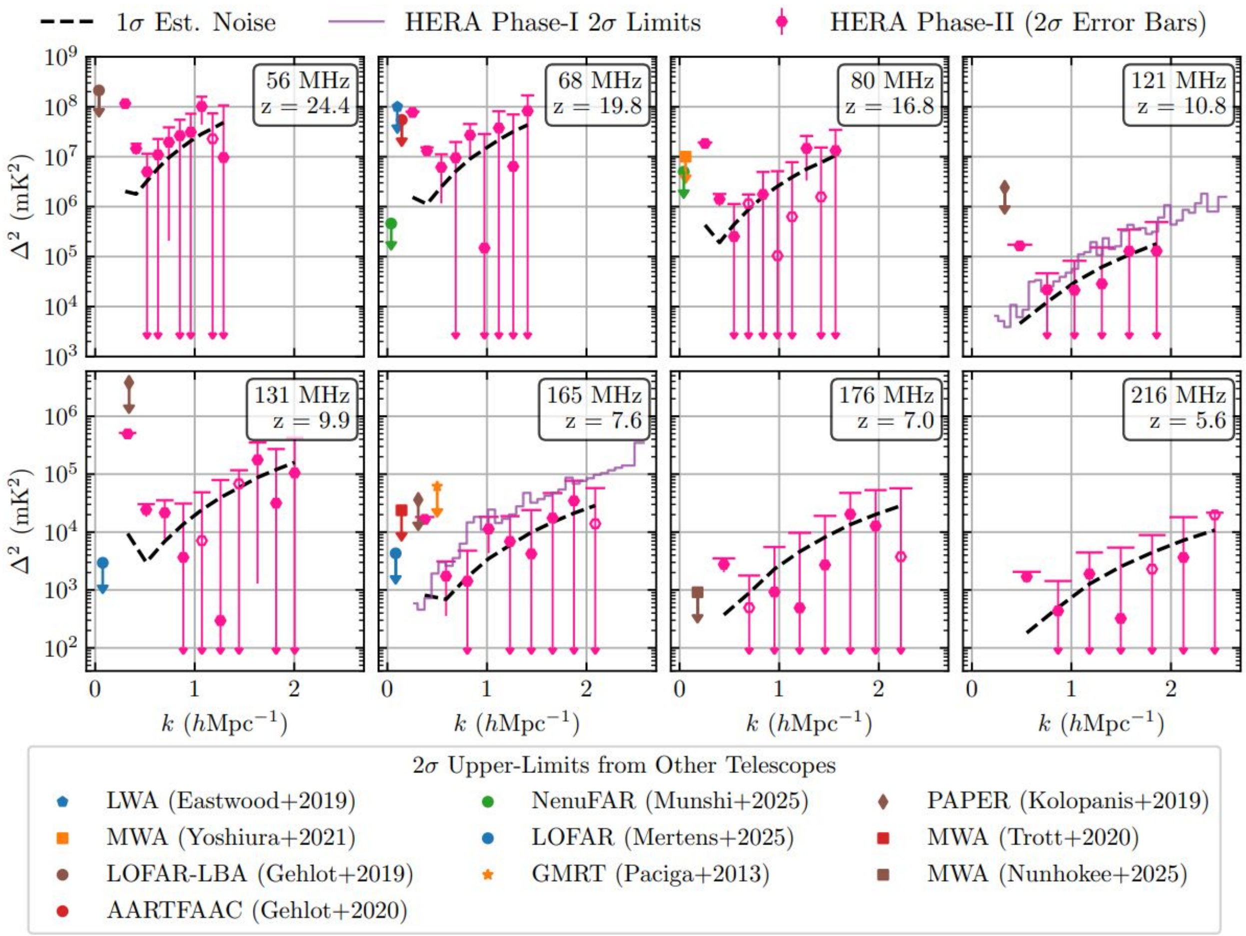

z = 5.3-24.4

Total time = 136.3 hr

HERA Phase II

Abdurashidova et al., 2025

Observational INFO

RFI & Noise

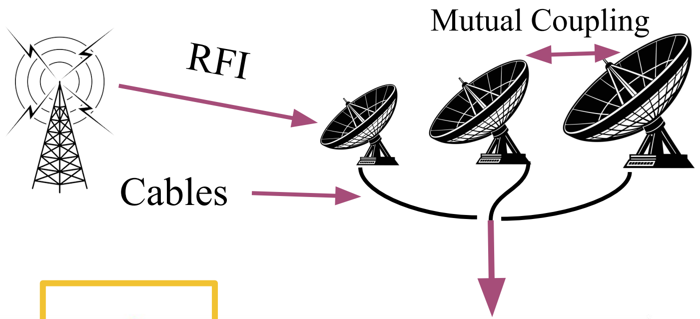

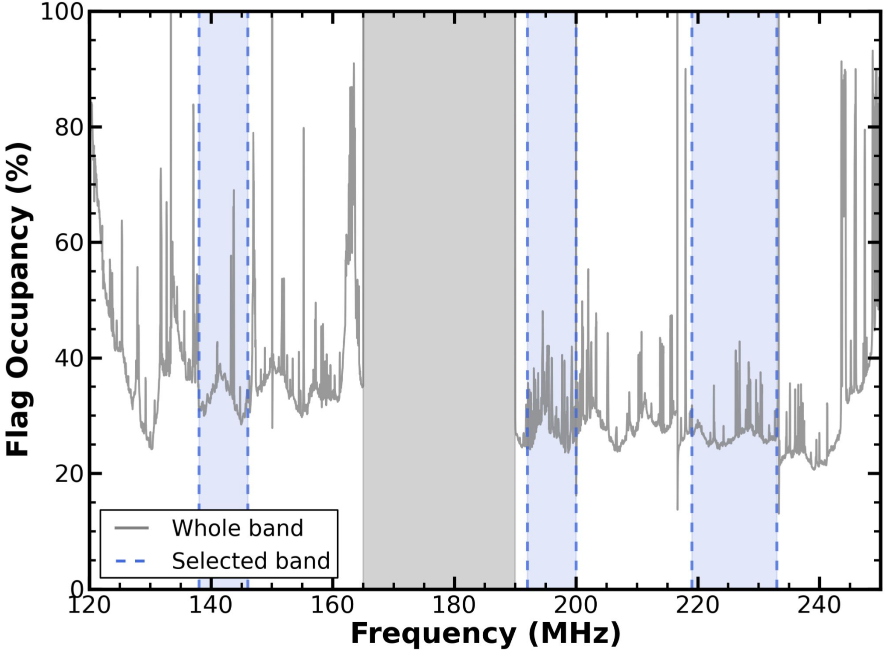

Sagar et al., (In prep.)

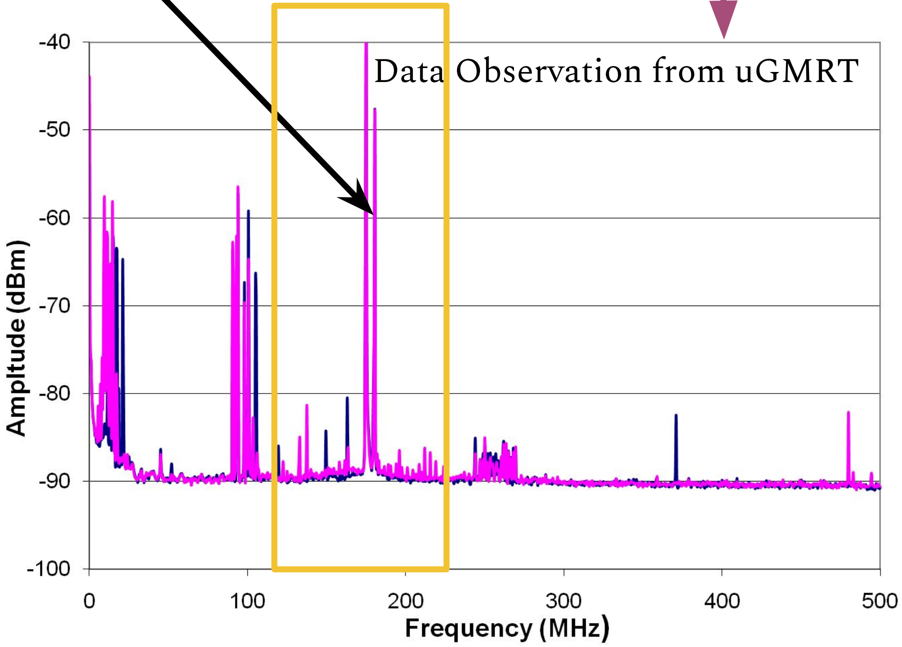

Raybole et al. 2010

Estimated residual Power Spectrum of HI 21-cm signal: multi-redshifts

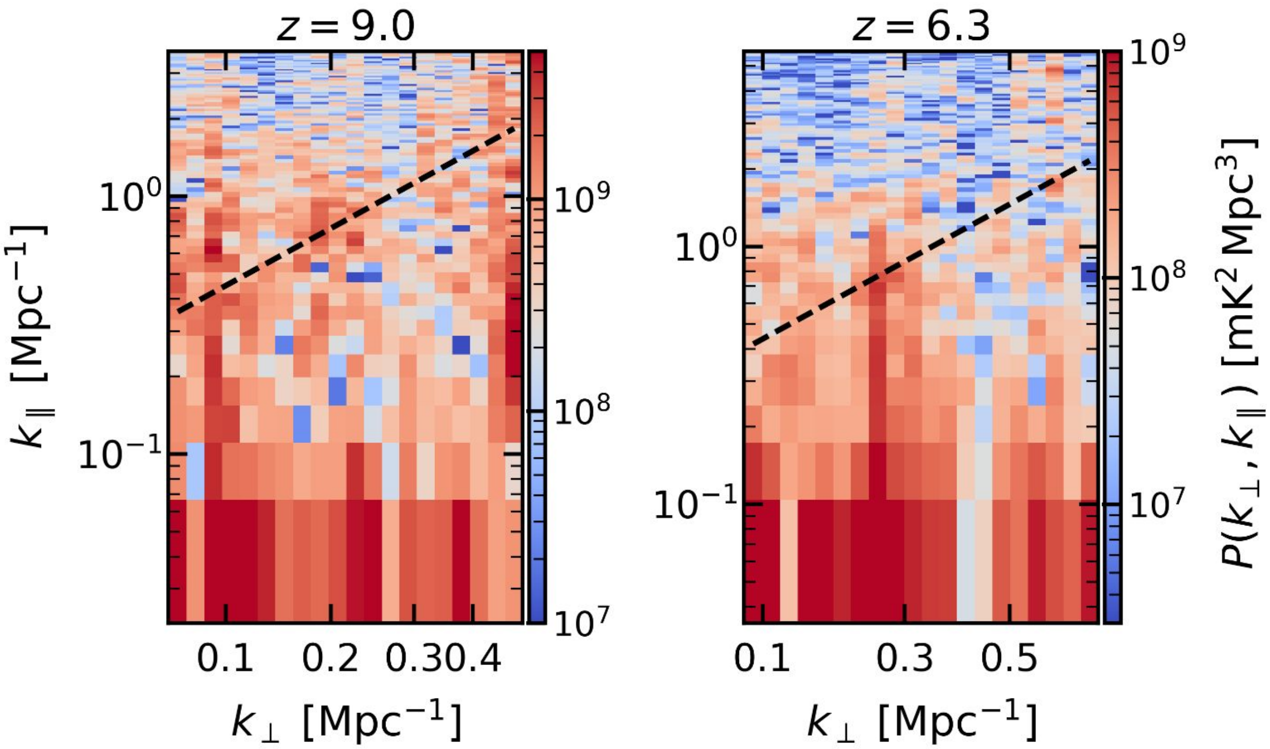

Sagar et al., (In prep.)

Estimated residual Power Spectrum of HI 21-cm signal: Foreground Avoidance

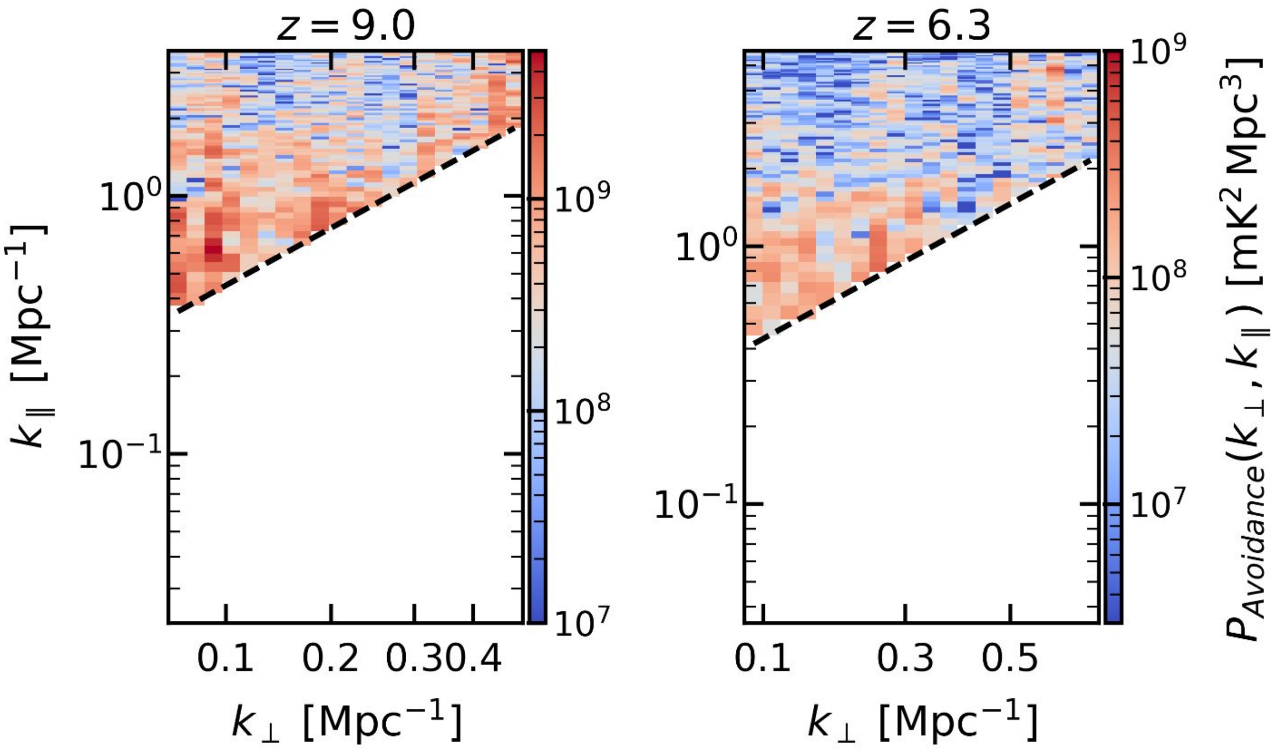

Sagar et al., (In prep.)

Estimated 3D Power Spectrum of HI 21-cm signal: multi-redshifts

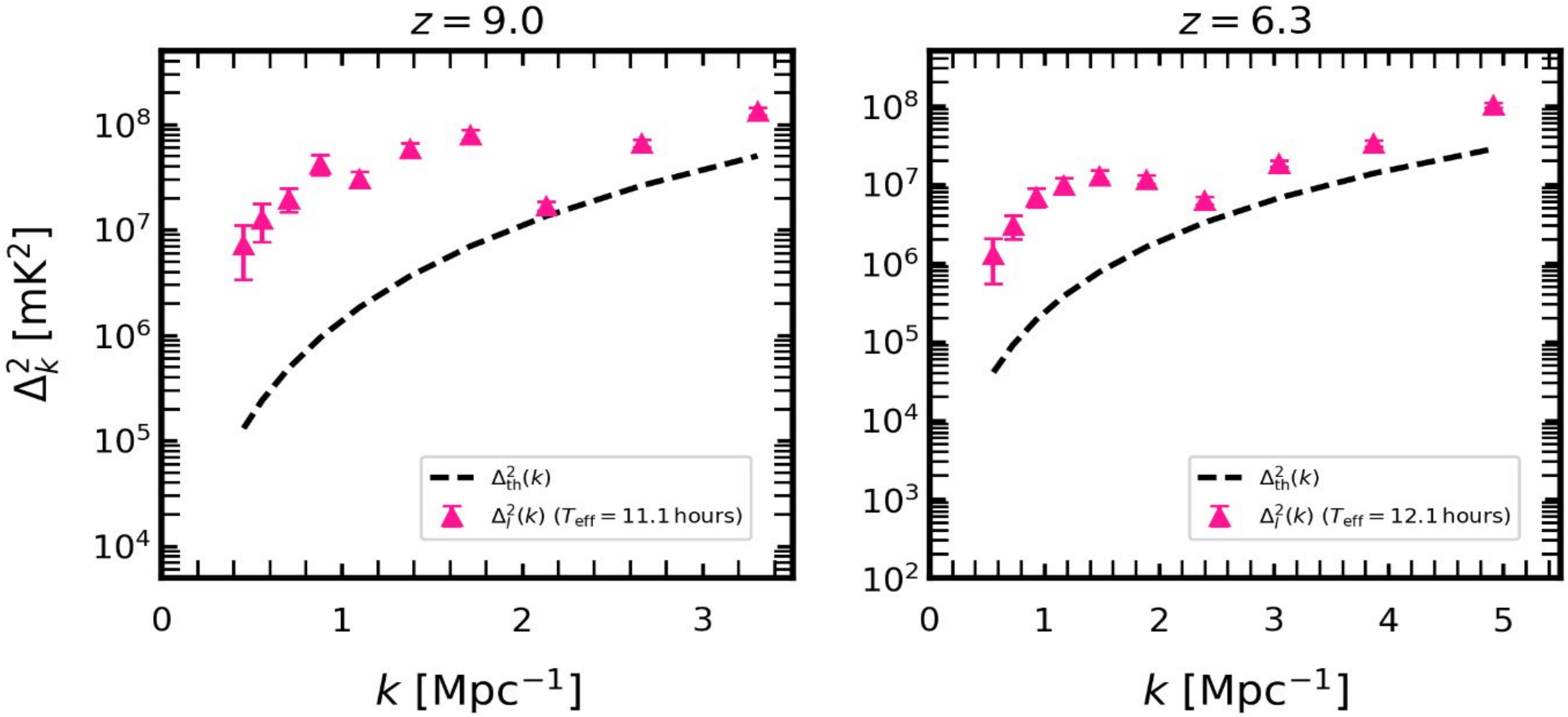

Sagar et al., (In prep.)

Estimated 3D Power Spectrum of HI 21-cm signal: multi-redshifts

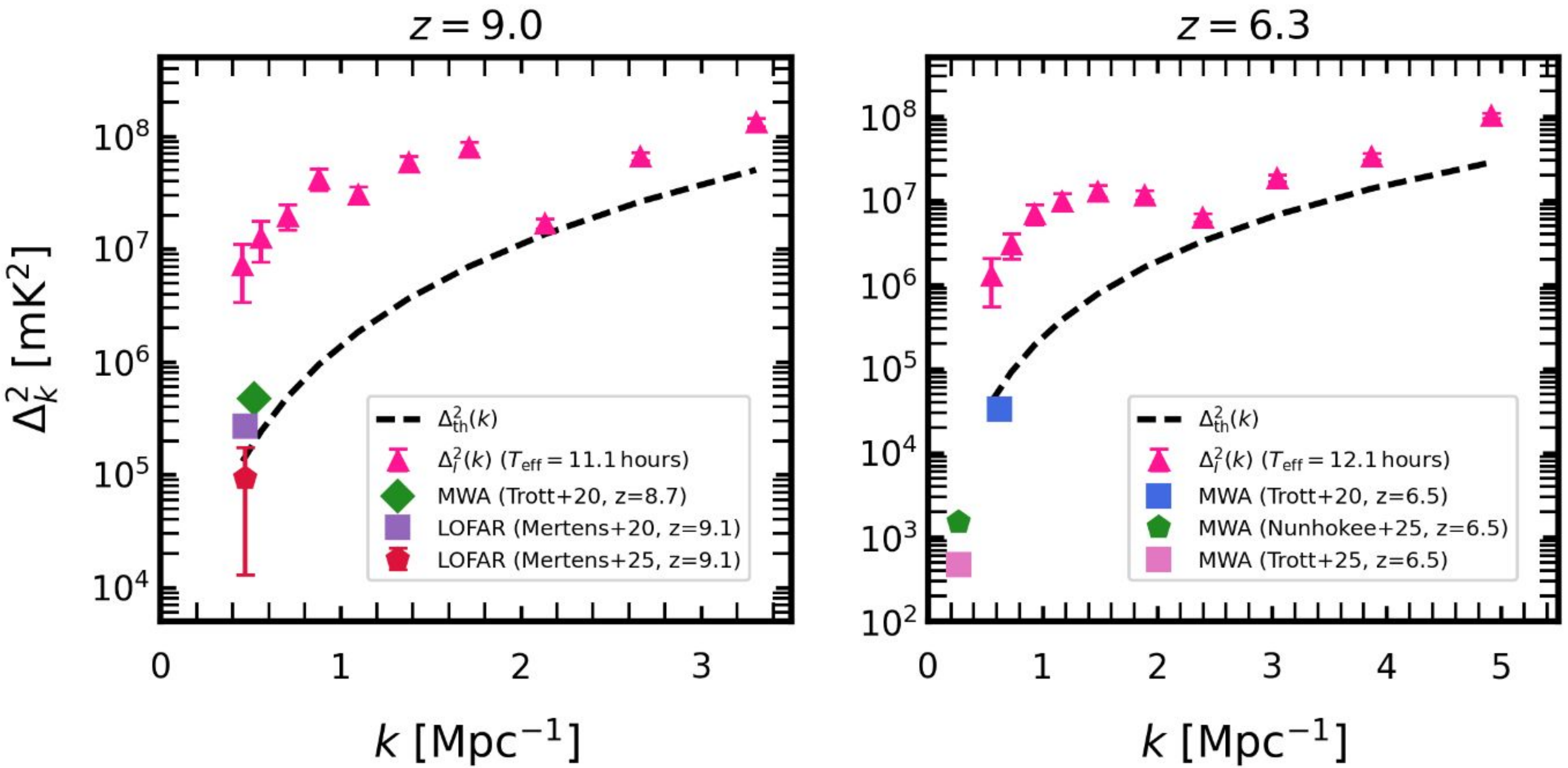

Sagar et al., (In prep.)

Estimated Power Spectrum of HI 21-cm signal: multi-redshifts

z	K (Mpc^{-1})	$\Delta^2(mK^2)$	$\Delta^2_{err}(mK^2)$	$\Delta^2_N(mK^2)$
6.3	0.556	$(1136.02)^2$	$(863.197)^2$	$(137.233)^2$
9.0	0.455	$(2686.026)^2$	$(1963.782)^2$	$(630.004)^2$

Sagar et al., (In prep.)

Summary

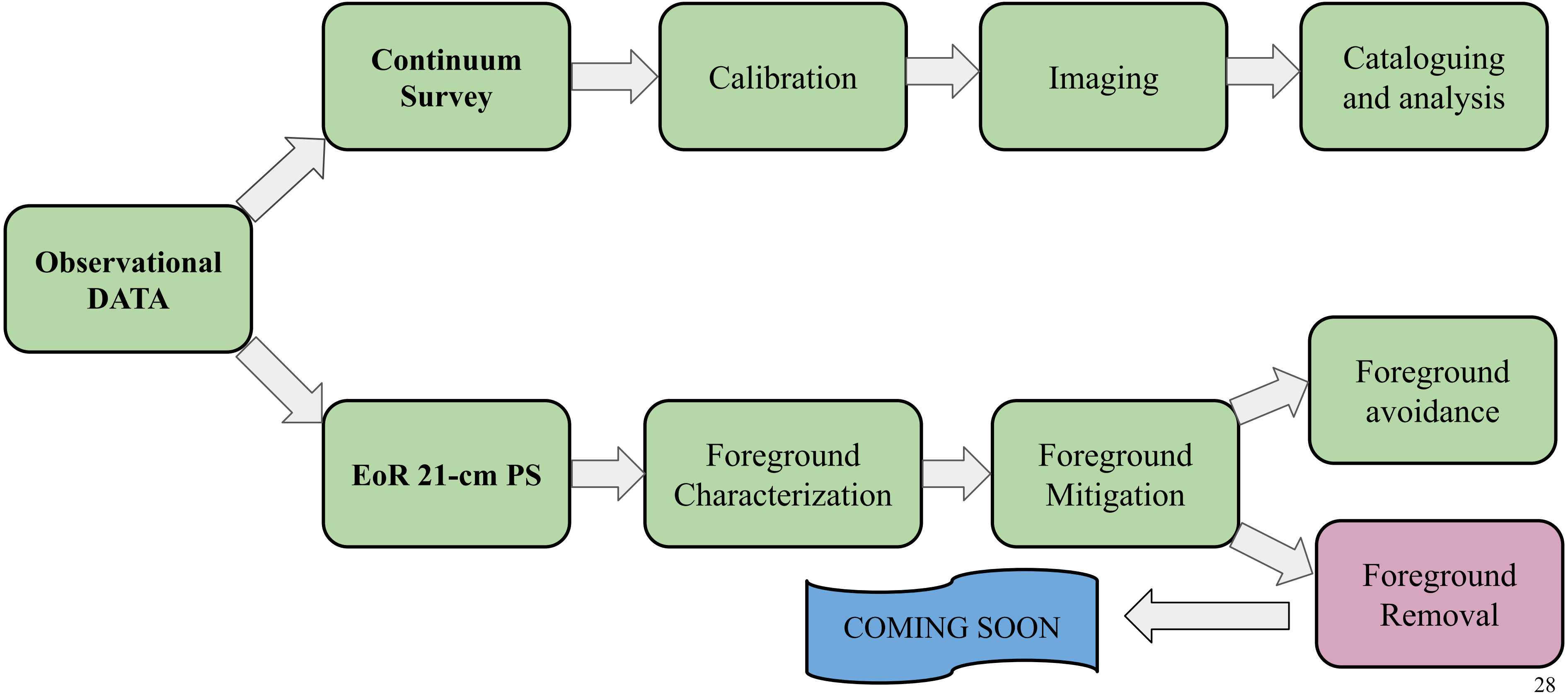
Continuum Survey
Calibration
Imaging
Cataloguing and analysis
Observational DATA
EoR 21-cm PS
Foreground Characterization
Foreground Mitigation
Foreground avoidance
Foreground Removal
COMING SOON

Current Generation Radio Interferometers: Study of Southern Sky

Continuum Imaging: GAMA-23 field with uGMRT Band-3

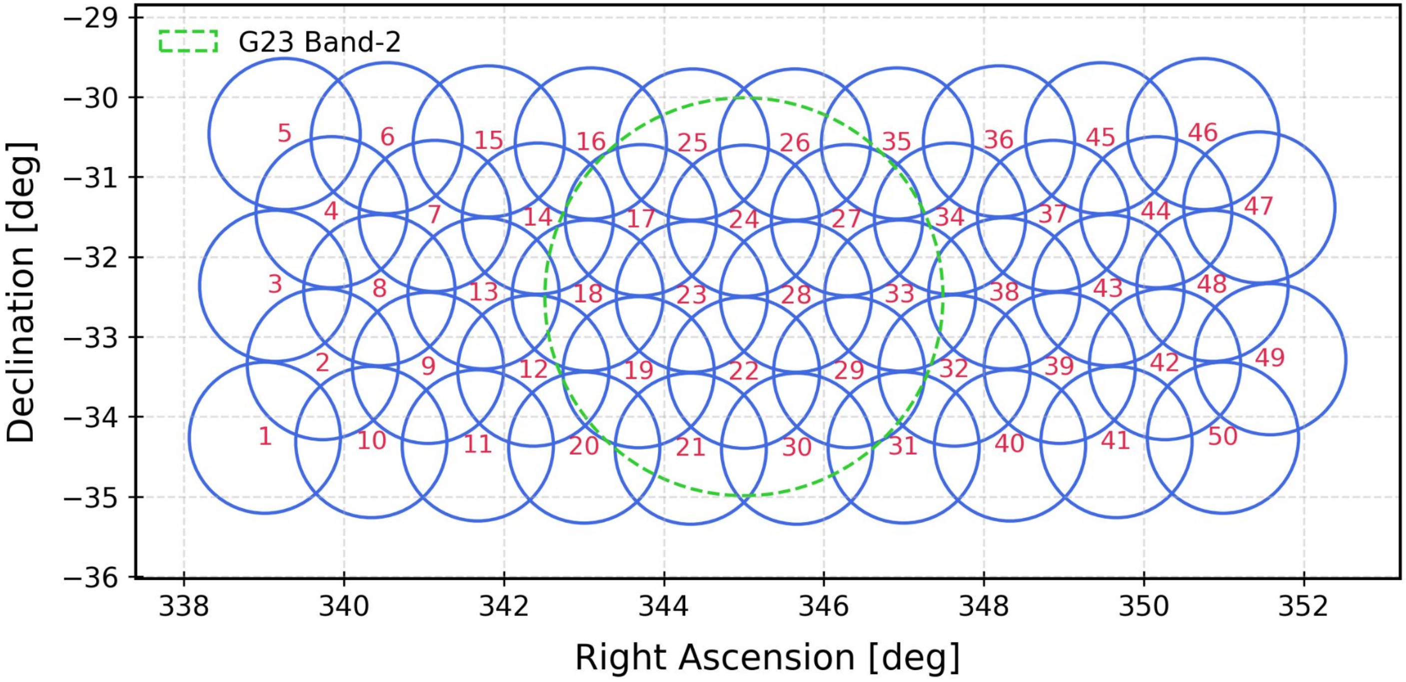

Observation = 33 hours
Pointings = 50

Sagar et al., (In prep.)

Continuum Imaging: GAMA-23 field with uGMRT Band-3

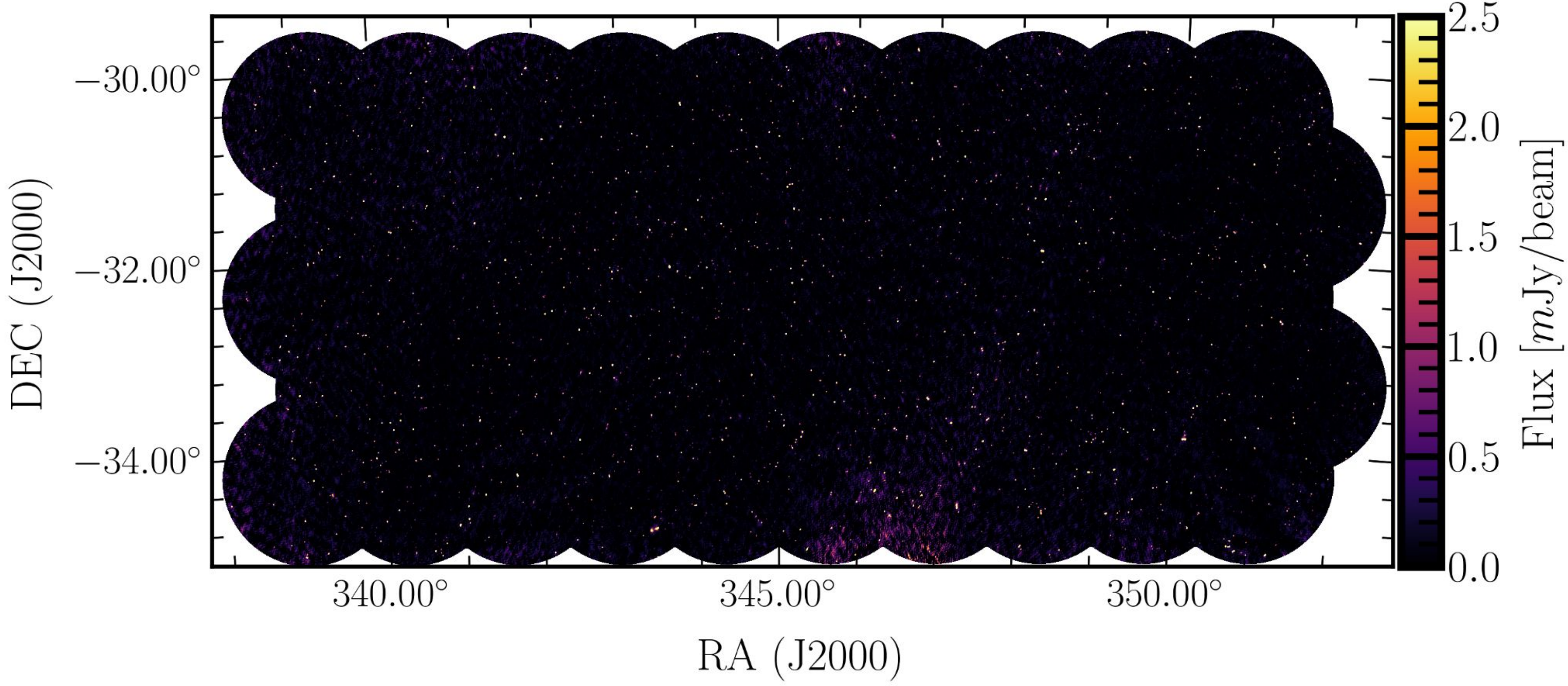

Sagar et al., (In prep.)

Observation = 33 hours
Resolution = 15.8”
RMS noise = 109 μJy/beam

Continuum Imaging: GAMA-23 field with uGMRT Band-3

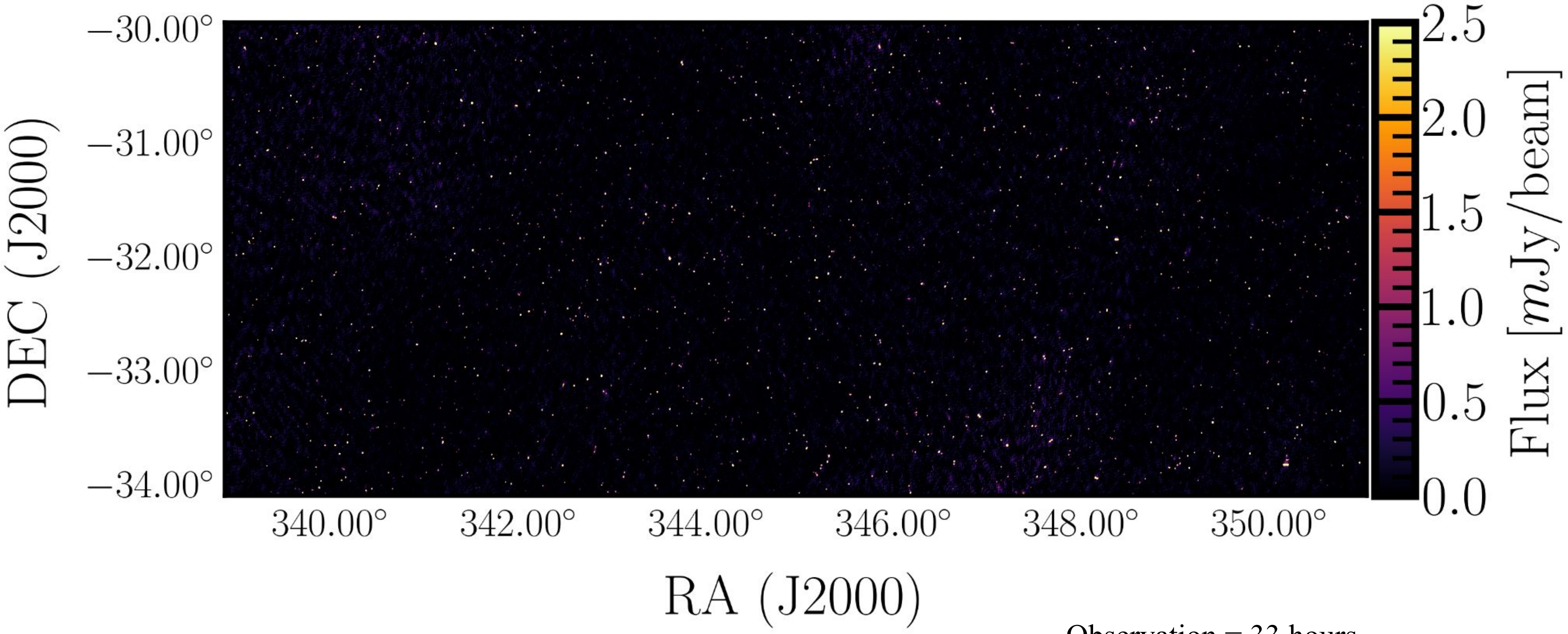

Sagar et al., (In prep.)

Observation = 33 hours
Resolution = 15.8”
RMS noise = 109 μJy/beam

Source Montage

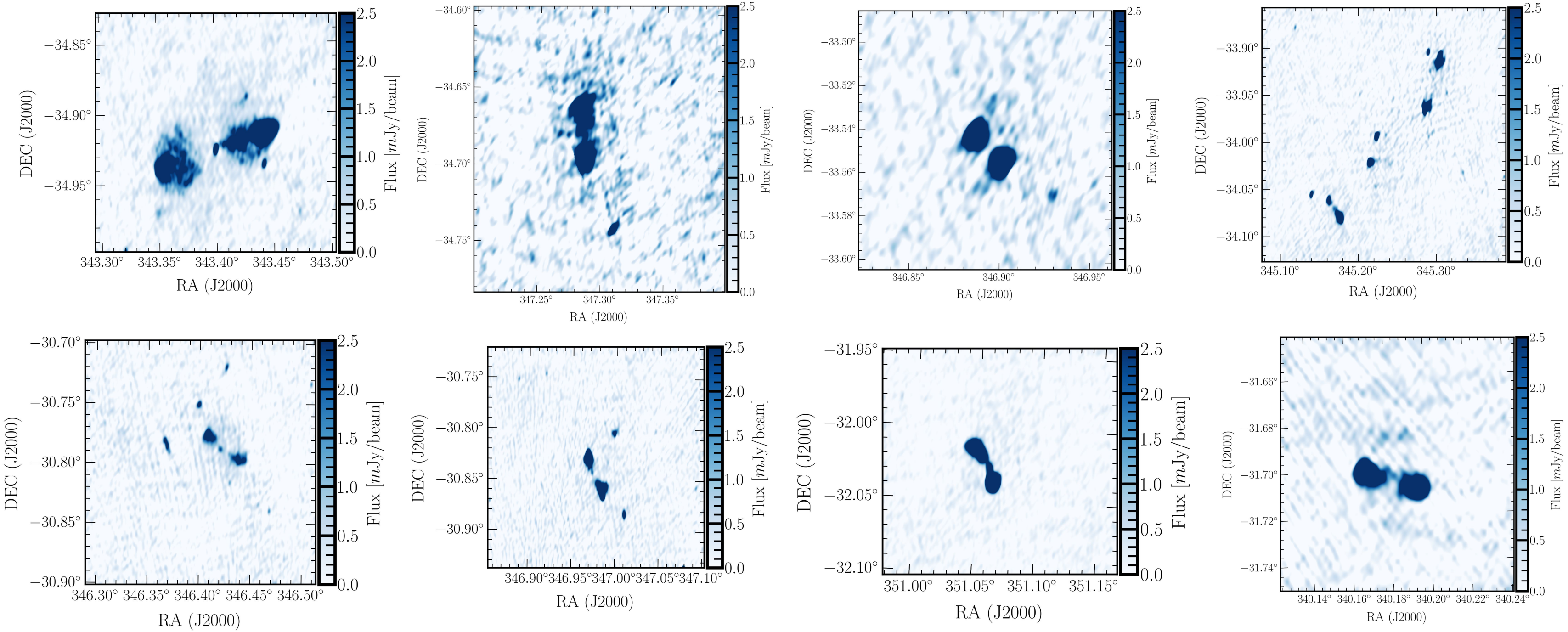

This Work